From high-purity synthesis to key experimental considerations for evaluating functionalized ionic liquids for combined capture and electrochemical conversion of CO_2

Saudagar Dongare[1], Eda Cagli[1], Oguz Kagan Coskun[1], Jared S. Stanley[2], Ab Qayoom Mir[2], Rowan S Brower[3], Jesús M. Velázquez[3], Jenny Y. Yang[2], Robert L Sacci[4], Burcu Gurkan[1,*]

[1]Department of Chemical and Biomolecular Engineering, Case Western Reserve University, Cleveland, OH

[2] Department of Chemistry, University of California, Irvine, CA

[3] Department of Chemistry, University of California, Davis, CA

[4] Chemical Sciences Division, Oak Ridge National Laboratory, Oak Ridge, TN

* Corresponding Author: beg23@case.edu

ABSTRACT

Ionic liquids (ILs) are considered functional electrolytes for the electrocatalytic reduction of CO_2 (ECO_2R) due to their role in the double-layer structure formation and increased CO_2 availability at the electrode surface, which reduces the voltage requirement. However, not all ILs are the same considering the purity and degree of the functionality of the IL. Further, there are critical experimental factors that impact the evaluation of ILs for ECO_2R including the reference electrode, working electrode construction, co-solvent selection, cell geometry, and whether the electrochemical cell is a single compartment or a divided cell. Here, we describe improved synthesis methods of imidazolium cyanopyrrolide IL for electrochemical studies in consideration of precursor composition and reaction time. We explored how IL dilution within acetonitrile, dimethylformamide (DMF), dimethyl sulfoxide (DMSO), propylene carbonate (PC), and n-methyl-2-pyrrolidone (NMP) affected conductivity and CO_2 mass transport, and ECO_2R activation overpotential, as well as surveyed effects of electrode material (Sn, Ag, Au and glassy carbon).

Acetonitrile was found to be the best solvent for lowering the onset potential and increasing the catalytic current density for the production of CO owing to the enhanced ion mobility in combination with the silver electrode. Further, the ECO_2R activity of molecular catalysts $Ni(cyclam)Cl_2$ and iron tetraphenylsulfonato porphyrin (FeTPPS) on carbon cloth electrode maintained high Faradaic efficiencies for CO in the presence of the IL. This study presents best practices for examining non-traditional multifunctional electrolytes amenable to integrated CO_2 capture and conversion technologies for homogenous and heterogenous ECO_2R.

INTRODUCTION

There are limited options for solvent/electrolyte combinations for combined capture and electrochemical conversion of CO_2. Aqueous electrolytes[1, 2] have low CO_2 solubility and suffer from a limited electrochemical window, thus resulting in hydrogen evolution reaction (HER) competition with the CO_2 reduction reaction ECO_2R. Organic electrolytes[2] that are composed of molecular solvents and supporting salts also present limited CO_2 solubility in addition to being flammable and highly volatile. Ionic liquids (ILs)[3, 4] are the only class of solvents that are not limited by the same competing reactions or low CO_2 solubility for a combined capture and conversion process. ILs are salts that melt below 100 °C; they have very low or negligible vapor pressures and high electrochemical stability.[5]

Many non-functional ILs are commercially available;[6] however, functionalized ILs tuned for specific applications are often not. Even with commercial ILs, the presence of trace level of impurities (e.g., moisture, metal-ions, or halides) negatively impact electrochemical stability and other physical properties, thus making it difficult to reproduce data and accurately interpret experimental results.[7] A simple protocol to functionalize ILs involves replacing the halide of the salt precursor or even a non-functional IL with an organic or inorganic anion bearing the functional moiety.[8] Alternatively, the functional moiety maybe appended to the cation through alkylation.[9] The former can be achieved via direct mixing or using ion exchange methodologies. Typically, higher purity is achieved by anion exchange via column chromatography followed by a metathesis reaction. These protocols have not been optimized for scalable functional IL synthesis with the high purity that is required for electrochemical studies. Here, the reaction times and stoichiometry were examined for improving the larger scale synthesis of 1-ethyl-3-metylimidazolium 2-cyanopyrrolide, [EMIM][2-CNpyr], which has been demonstrated as a superior IL in terms of CO_2

capture capacity under low partial pressures[10, 11] and ECO_2R performance for CO_2-to-CO over Ag[12] and CO_2-to-C_{2+} over Cu[13] electrodes. As such functional ILs present unique behavior near polarized surfaces, it is also imperative to perform ECO_2R with appropriate techniques and careful analysis that allow comparisons of the catalytic behavior in the IL.

One of the earliest examined ILs for ECO_2R is the commercially available imidazolium tetrafluoroborate, $[EMIM][BF_4]$.[4] This IL was shown to reduce the energy requirement of the formation of $CO_2^{\bullet-}$ anion radical, which is the believed to be the first and rate-determining step (RDS) in the mechanism for ECO_2R. Further, this IL was shown to stabilize the reaction intermediates on electrode surface, thus enhancing ECO_2R selectivity while suppressing competitive HER.[14] Since then, imidazolium based ILs have been examined for ECO_2R and have demonstrated selective for CO production on Ag working electrode.[15, 16] However, for practical ECO_2R studies, the viscosity of neat ILs is too high (typically > 20 cP at 25 °C); moreover, the viscosity of the functionalized ILs increase with CO_2 saturation, thus limiting current response and product yield. Therefore, organic solvents were utilized as dilutants in IL electrolytes to enhance ECO_2R performance.[17] Recent studies highlighted the significant influence of the electrolyte composition on the rates of CO_2 reduction and H_2 evolution.[2]

When examining the influence of the electrolyte composition, purity is an important criteria since metal-ion or halide impurities (e.g., Pb^{2+},Cl^-, Br^-, and I^-) are shown to deactivate the electrode due to deposition of these impurities during electrolysis, blocking catalytic active sites and promoting HER.[18] Further, water is a common impurity in IL electrolytes due to the hydrophilicity of the IL; trace amount of water is often unavoidable even with careful sample preparation and handling.[19] Recently, Guo et al.[20] studied the ECO_2R kinetics in $[EMIM][BF_4]$/acetonitrile electrolyte with varying the water content from 0.03 to 1.01 M on Ag, where the primary ECO_2R product was CO

(~85 % FE with 0.03 M water). However, the formations of H_2 and formate are reported at higher water content due to the change in interfacial microenvironment caused by water. Although not IL based, Figueiredo et al.,[21] examined the microenvironment in a 0.1 M tetraethylammonium tetrafluoroborate ([TEA][BF_4])/acetonitrile electrolyte containing trace amounts of water on Cu by an in-situ FTIR spectroscopy. The primary ECO_2R product was CO; however, the formation of bicarbonate and carbonate were also suggested, and the amount produced was influenced by the residual water. The formation of carbonate and bicarbonate species seems to result from a solution-phase reaction of CO_2 with electrochemically generated OH^- from the water reduction. Therefore, even a residual amount of water maybe relevant to examine in ECO_2R with nonaqueous electrolytes, including ILs that are usually hygroscopic.

Besides electrolyte composition and the choice of the electrode, the configuration of the electrochemical cell stands as a critical parameter impacting mass transport behavior that ultimately influences the feasibility of ECO_2R.[22] Most of the fundamental science studies use electrochemical cells with stationary electrolytes whereas practical applications or applied research use cells with flowing electrolytes. There is variability in electrode placement in static cells and varied flow conditions in flow cells. Therefore, there is inconsistency with comparing the results between the reactive systems that operate on widely varied length and time scales. Lastly, one must consider the selection of the analytical methodology for ECO_2R product quantification. For gaseous products, online methods such as gas chromatography (GC)[23] and differential electrochemical mass spectrometry (DEMS)[24] with their improved detection limits[25] are suitable.Liquid products can be quantified using high-performance liquid chromatography (HPLC)[17] or (for ionic species like formate) ion-exchange chromatography,[26] and nuclear magnetic resonance spectroscopy (NMR),[13] and combinations thereof. Among the quantitative online techniques, GC and NMR has been widely used due to their wide availability and ability to detect a broad range of products without any interference of the solvent, which can be problematic using DEMS.

While there has been a considerable number of reports detailing the study of heterogeneous electro-catalysis in ILs, there are fewer reports of homogeneous molecular electro-catalysis in ILs.[27-29] The presence of an IL with high CO_2 solubility increases the CO_2 availability in the vicinity of the molecular catalyst, which can have an impact on the rate of CO_2 reduction. These effects are underexplored within the homogeneous systems.

Here, we examined the influence of a reactive IL and the synergy between the IL and the model molecular catalysts on the homogenous and heterogenous electrocatalysis of CO_2. More specifically, we report an improved synthetic method for the preparation of imidazolium-based CO_2-reactive ILs with a basic anion as an example for increased purity and scalability for adaption in ECO_2R. As CO_2-reactive ILs typically present high viscosities and condensed interfacial behavior near the electrode, different organic solvents, listed in **Table 1**, are examined in terms of tuning of viscosity, conductivity, and CO_2 solubility. The impact of electrode material (Ag, Au, and glassy carbon) and electrochemical cell configuration on CO_2 reduction product distribution and electrolyte stability during ECO_2R were also investigated. Further, the molecular catalysts iron tetraphenylsulfonatoporphryin (FeTPPS) and nickel cyclam ($Ni(cyclam)Cl_2$ or $Ni(cyclam)^{+2}$) were studied in the presence of the IL for ECO_2R with a carbon cloth electrode. These represent common molecular catalysts in ECO_2R. The latter catalyst has high HER activity using carbon working electrodes under aqueous conditions.[30, 31] The hypothesis being probed in this study is the elimination of HER selectivity during ECO_2R facilitated by molecular catalysts in the presence of the IL in a polar aprotic solvent to achieve quantitative Faradaic yield for CO. In addition to these investigations, electrochemical methods better suited for the characterization of small-volume IL based electrolytes are discussed. This study aims to bring attention to the critical considerations when examining non-traditional multifunctional electrolytes that are amenable for integrated CO_2 capture and conversion technologies for ECO_2R.

Table 1: CO_2 solubility and physical properties of organic solvents used in the study,[32-35] in comparison the IL, [EMIM][2-CNpyr].[36] CO_2 solubility, viscosity, and vapor pressure are measured at 25 °C.

Solvent	**Co_2 Solubility (Mmol.Kg^{-1})**	**Viscosity (Mpa.S)**	**Vapor Pressure (Torr)**	**Boiling Point (°C)**
Acetonitrile	399	0.341	88.8	82
Dimethylformamide (DMF)	205	0.802	2.3	153
Dimethylsulfoxide (DMSO)	119	1.99	0.417	189
N-methylpyrrolidinone (NMP)	147	1.89	0.33	202
Propylene carbonate (PC)	112	2.53	0.13	242
[EMIM][2-CNpyr]	4573	67.8	N/A	N/A

EXPERIMENTAL

Materials

Anion precursor, pyrrole 2-carbonitrile (2-CNpyrH) (99%, Alfa Aesar) was used as received. Cation precursors, 1-ethyl-3-methyl imidazolium bromide ([EMIM][Br]), was synthesized from 1-methylimidazole (>99%, TCI) and bromo ethane (99%, TCI) while 1-ethyl-3-methyl imidazolium chloride ([EMIM][Cl], 98%, Sigma Aldrich) was used as received and dried under vacuum at 60 °C. Hydroxide-form anion exchange resin (AER) (A600-OH, Purolite) was packed into the column and washed with methanol prior to use. Cation exchange membrane, Nafion-117 was purchased from Fuel Cell Store, USA. As received Nafion-117 pretreated with H_2O_2 and H_2SO_4 to remove organic impurities and improve the proton conductivity, respectively. The detailed Nafion-117 pretreatment procedure is reported elsewhere.[37] The pretreated Nafion-117 membrane was stored in 0.1 M tetraethylammonium perchlorate/acetonitrile solution.

Other chemicals, including silver nitrate (0.171N, Ricca), methanol (99.8%, HPLC grade, Fischer), acetonitrile (99.8%, HPLC grade, Fischer), and DMSO-d6 (99.9%, Thermo Scientific) were used as received. For the supporting electrolyte, as received tetraethylammonium perchlorate (TEAP, ≥ 98%, BeanTown Chemical) was dried overnight at 100 °C under vacuum to remove trace volatiles. For nuclear magnetic resonance (NMR) spectroscopy (Bruker Ascend 500MHz), dimethyl sulfoxide-d6 (DMSO-d6, 99.9% (Isotopic), Thermo Scientific) was used in sample preparation. Iron tetraphenylsulfonato porphyrin (FETPPS) was purchased from Frontier Scientific and used as received. 2,2,2-Trifluoroethanol (TFE) and tetrabutylammonium hexafluorophosphate ($TBAPF_6$) were purchased from TCI. $TBAPF_6$ was recrystallized three times from ethanol. Ni(cyclam)Cl_2 was synthesized according to the reported method.[30]

Modified IL synthesis procedure

Reaction conditions were improved to facilitate the scalable IL synthesis while considering the purity through the modification in reaction time, starting material stoichiometries, and solvent use. First, cation precursor, 1-ethyl-3-methylimidazolium bromide ([EMIM][Br]), was synthesized by solventless quaternization/Menshutkin reaction between methyl imidazole and ethyl bromide. The purity of [EMIM][Br] was confirmed by ^{1}H-NMR spectrum (Figure S1). The dried [EMIM][Br] was then converted to [EMIM][2-CNpyr] following the previously reported procedure[36, 38] with some modifications. One of the specific modifications is the use of an anion exchange column (¾ diameter and 25-inch height; filled with the resin with a quartz wool plug) which is preferred over batch treatment for scalable synthesis. The use of an anion exchange column offers several advantages in terms of reducing the amount of resin, organic solvent and time required. Further, it helps prevent the crushing of resin beads due to stirring and enhances process efficiency by creating a concentration gradient[39]. A slurry of anion exchange resin in methanol was poured into the column to fill. The column was allowed to equilibrate for 15 min before adding the [EMIM][Br] (0.03 mmol for a 6 gram IL batch) solution which was fully dissolved in the minimum volume of methanol (~1-2 mL). The solution was placed carefully on top of the column and allowed to elute through column with a steady flow of 3 mL/min. The [EMIM][OH] solution was then collected from the bottom of the column after ca. 45-60 mins and was subjected to silver nitrate test. Conversion of [EMIM][Br] to [EMIM][OH] was verified by the lack of precipitation upon adding a few drops of the silver nitrate solution (0.014 M) to the aliquot collected from the anion exchange column (~1-2 mL), confirming the halide content to be less than 140 ppm. The obtained [EMIM][OH] solution in ca. 0. 2 mM was concentrated up to 0.5 M with the use of rotary evaporator. Note that, further concentrating this solution beyond 0.5 M leads to its degradation in highly alkaline environment.[40] The ^{1}H NMR spectrum of 0.5 M [EMIM][OH]/methanol solution is shown in Figure S1. Then, the equimolar amount of pyrrole 2-carbonitrile was added and the solution was magnetically stirred effectively at 22 °C for 24 hours under atmospheric conditions. The aliquots from the synthesis solution were collected after 1, 2, 3, 4, and 24 hours to determine the minimum required reaction time. At each time interval, aliquots were collected for NMR and FTIR analysis. After completion of the reaction, the solvent (i.e., methanol) was removed via rotary evaporation and water formed during the synthesis was further removed by vacuum drying at 45-50 °C for 3 hours under continuous effective stirring. Finally, IL (6 grams) was obtained as a liquid and its structure was again verified by ^{1}H-NMR and FTIR.

After confirming the successful IL synthesis with minimal impurity, we then scaled up the synthesis batch to 40 gram using the necessary starting materials (0.2 mmol of [EMIM][Br] and equimolar amount of pyrrole-2-carbonitrile). The final halide impurity was further determined by combustion ion chromatography (by Atlantic Microlab Inc.) where it was found to be lower than the detection limit of 0.25%. In addition, elemental analyses (Atlantic Microlab Inc.) of [EMIM][2-CNpyr] synthesized from [EMIM][Br] showed 60.47% (60.52%) carbon, 7.40% (7.23%) hydrogen, 25.40% (25.35%) nitrogen. The same procedure was repeated with the starting material of [EMIM][Cl] and the elemental analysis showed 61.20% (61.10%) carbon, 7.19% (7.17%) hydrogen, 25.81% (25.65%) nitrogen. The analyses were duplicated, and the duplicate results are shown in parenthesis for comparison. The elemental analysis results are in good agreement with the theoretically calculated values, further confirming the efficiency of the synthesis and minimized impurity in IL. The water content was measured by Karl-Fischer titration and was found to be below 500 ppm.

Electrochemical Methods

Linear sweep voltammetry (LSV): Unless otherwise noted, all voltammetric measurements with diluted IL solutions were performed in a 5 mL single-compartment three-electrode cell (Pine Research, USA) with a Bio-Logic VSP-300 multichannel potentiostat. A standard disk electrode (glassy carbon, Ag, and Au; purchased from BASi) with 1.6 mm diameter was used as the WE. LSVs with tin (Sn, 98.8 %, Millipore Sigma) were performed with 2X2 mm sheet. Prior to experiments, the disk electrodes were polished with a 0.30 μm fine alumina suspension (PINE research), then rinsed with ultrapure water, followed by sonication in ultrapure acetonitrile. A Pt wire was used as the counter electrode and non-aqueous Ag/Ag^+ was used as the reference electrode. The reference electrode was prepared by immersing polished Ag wire into an 0.1 M TEAP/acetonitrile containing 10 mM $AgNO_3$ with a porous frit at one end.

T-cell voltammetry: Considering the sensitivity of ILs towards moisture, the electrochemical window of the pure IL was measured using cyclic voltammetry (CV) in an air-tight T-cell[41] configuration with minimized sample size (see **Figure 1a)**. Accordingly, the required IL volume can be as low as 20 to 200 μL, depending on the size of the reference electrode. The atmosphere can be controlled by having a flow of a dry inert gas, thus eliminating the effects of water and dissolved reactive gases. A small portion of a plastic disposable pipette tip or a heat-shrink tube fitted to the electrode diameter was securely placed around the end of the working electrode (Ag disk, 1.5 mm) to create a cavity within which 200 μL of the IL sample was placed. The reference electrode (Ag/Ag^+) and counter electrode (Pt wire) were immersed from the top as shown in **Figure 1a**. This configuration allows the placement of the reference electrode close to the working electrode.

The micro-voltammetry experiments with the Ag microelectrode (dia. 12µm (area-1.23×10^{-6} cm^2), BaSi) were conducted in 0.1 M [EMIM][2-CNpyr]/acetonitrile electrolyte with 0.1 M TEAP supporting salt in a T- cell with the three-electrode setup described above. The cell was placed in a Faraday's cage on an isolating surface (i.e., a sponge) to avoid any external disturbances on the electrochemical signal collected from micro-voltammetry (e.g., external electromagnetic fields or vibrations present in the lab environment). Prior to the experiments, the microelectrode was sonicated in an acetonitrile solution for five minutes to ensure a clean surface.

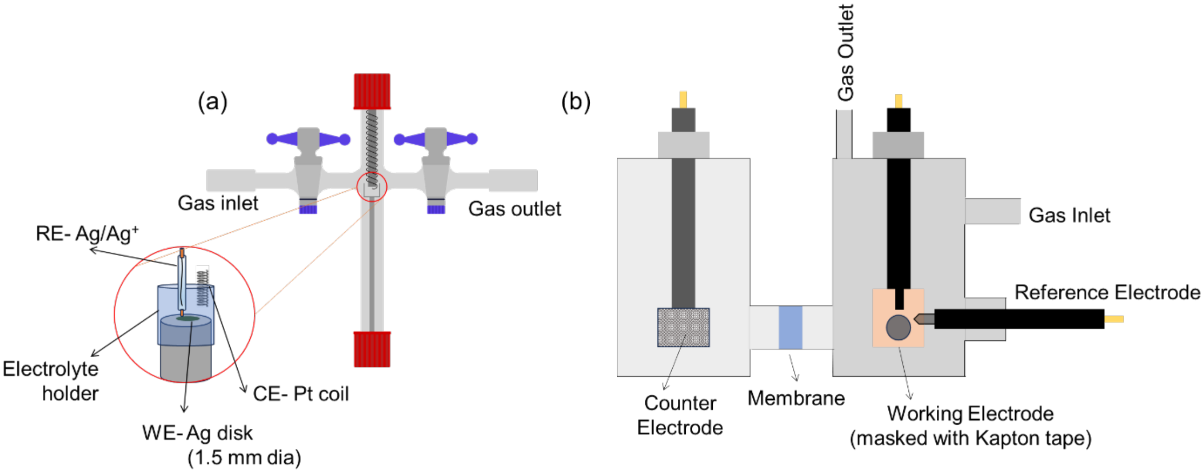

Figure 1: (a) Cross section of the low volume T-cell employed for cyclic voltammetry and micro-voltammetry measurements using 200 µL electrolyte sample under controlled gas atmosphere conditions; **(b)** Schematics of two compartment H-cell used for bulk electrolysis experiment a minimum amount of electrolytes (5 mL) where the distance between working and counter electrode was 5 cm.

Dynamic impedance: The double layer capacitance was dynamically measured using dynamic electrochemical impedance spectroscopy (DEIS). The instrumentation details and the experimental setup has been described previously[42] and only a brief description is given here. A multisine waveform consisting of 45 frequencies between 37.5 kHz to 1 Hz was synthesized by a waveform generator. Briefly: (1) each frequency in the waveform had an integer number of periods in the waveform period, $T = 1/f_{\min}$; (2) frequencies are based on Popkirov's prime number selection rule that is then multiplied by $f_{\min}$ to reduce harmonic and interharmonic overlap; (3) the amplitude for individual waves decreased by half for every decade increase in the frequency; (4) the phases of individual waves were randomized; and (5) the maximum amplitude of the ac waveform was ~35 mV. The waveform was fed into a Biologic potentiostat (SP-240) and was added atop the cyclic voltammogram protocol. After measurement, the raw data was transformed into the frequency domain using a sliding Fast Fourier Transform algorithm which was then converted to complex impedance (*Z*) *via* Eq. (1):

$$Z = \frac{(E_r I_r + E_i I_i) + \mathrm{i}(E_i I_r - E_r I_i)}{(I_r^2 + I_i^2)} \qquad \text{Eq. (1)}$$

where *E* for potential, *I* for current, *r* and *i* are for real and imaginary, respectively. We extracted only the frequencies that corresponded to those used in the multisine waveform that was applied to the system. We only fit frequencies between 0.1 and 37.5 kHz to a standard Randel's circuit to extract the double layer capacitance value. For these measurements the cell was a ¼ inch T-cell with 2 mm Ag CH Instrument working electrode and 1/4inch dia. polished graphite counter electrode and an Ag/AgCl reference electrode.

H-cell electrolysis: The bulk electrolysis experiments was performed in a two-compartment H-type cell separated by Nafion-117 cation exchange membrane (Fuel Cell Store, USA) (**Figure 1b**). The cathodic chamber contained the working electrode (Ag Foil, ≥99.9%, area- 0.44 cm^2, thickness 1.0 mm, supplied by BeanTown Chemical) and the same reference electrode (Ag/Ag$^+$) described previously. The anodic chamber housed the counter electrode: Pt mesh (99.9%, 2 X 2 cm, BASi Research Products) or carbon rod (6 mm dia., BASi Research Products). The distance between working and counter electrodes was 5 cm. The working electrode chamber was continuously stirred, and CO_2 gas (10 sccm) was fed through the overhead of the catholyte chamber to ensure sufficient CO_2 availability in the electrolyte. It should be noted that bubbling of CO_2 through the catholyte was avoided since it could lead to uneven flow at the H-cell outlet, potentially resulting in incorrect interpretations when calculating the product selectivity. The gaseous products sampled from the overhead of the catholyte chamber were analyzed with the online gas chromatography (GC) (Agilent, 7890B) equipped with flame ionization detector (FID) and thermal conductivity detector (TCD). The liquid product was analyzed by ^{1}H and ^{13}C NMR spectroscopy after electrolysis. Since most of the H-cell electrolysis experiments were performed with 0.1 M IL concentration, NMR samples were prepared by mixing 350 μL of DMSO-d6 solvent with 350 μL of electrolyte. In the case of pure IL NMR sampling, only 30 μL IL in 720 μL of DMSO-d6 solvent was used for NMR quantification.

The Faradaic efficiency (FE) for ECO_2R gaseous products during the electrolysis experiments was calculated as follows, Eq. (2):[43]

$$\mathrm{FE}\ (\%) = \frac{e_{output}}{e_{input}} \times 100 = \frac{\left(V/_{V_m}\right)YN}{\left(V/_{v}\right)It/F} \times 100 \qquad \text{Eq. (2)}$$

where, e_{output} is number of electrons required for ECO_2R, e_{input} is number of electrons measured during sampling period, V is volume of GC sampling loop (mL) (0.25 mL for CO and 0.1 mL for H_2), V_m is ideal molar gas volume (22.4 L/mol), N (=2) is the number of electrons required to form CO or H_2 (possible ECO_2R products with Ag electrode), F is the Faraday constant (96,485 C/mol), and I is the recorded current. The flow rate of CO_2 was $\nu = 10$ mL/min. The measured amount of product (Y in units of mol) in a 0.25 mL sample loop was then calculated using the corresponding calibration curves of the GC that were previously developed using standard gases.[12]

Ionic conductivity and viscosity measurements: Ionic conductivity (σ) measurements were performed using electrochemical impedance spectroscopy (EIS).[44] Two platinized platinum electrodes (BioLogic USA) were immersed in a sample solutions and impedance measurements were performed at 100 Hz to 100 kHz to with 5 mV voltage amplitude at 25 ±0.2 °C. The solution resistances of the samples were then determined from the intercept of the high frequency data with the real resistance axis in a Nyquist plot. Using the measured resistance, the conductivity was calculated using the Eq. (3).

$$\sigma\ (mS.cm^{-1}) = \frac{k\ (cm^{-1})}{\rho\ (ohm)} \times 10^3 \qquad \text{Eq. (3)}$$

where σ is the ionic conductivity of the sample, *k* the cell constant, and ρ is the solution resistance determined from Nyquist plot. The cell constant of the platinized cell was measured with 0.1 M KCl before each measurement.

Viscosity measurements were performed with a microchannel viscometer (Rheosense; MicroVISC) in a temperature control unit maintained at 25 ± 0.2 °C. A single measurement required approximately 15 μL of sample. Before testing each sample, the microchannel chip was rinsed with methanol followed by deionized water. The viscosity of N100 and S20 standards (supplied by Cannon Instrument company) were measured at 25 ± 0.2 °C to confirm the reliability of measurements and found to be within 0.2%. Viscosity measurements were repeated three times and an average is reported.

Electrochemical characterization with molecular catalysts: Electrochemical techniques were performed using a Pine Wavedriver 10 bipotentiostat under an inert argon atmosphere unless otherwise noted. All solutions were internally referenced to $Fe(C_5H_5)_2^{+/0}$. Electrolysis was performed in a custom H-cell with a gas bridge, with a 19 mL working compartment, 10 mL counter compartment separated by a porous glass frit with a gas bridge of 1 ml approx. The working and counter compartments were sealed using GL25 and GL18 open top caps with silicone/PTFE septa from Ace Glass.

CV measurements with FeTPPS and Ni(cyclam)Cl_2 molecular catalysts were carried out with a 1 mm glassy carbon disk working electrode, a glassy carbon rod counter electrode, and a silver wire reference electrode. All CVs were scanned cathodically in a dry propylene carbonate solution containing 0.1 M [EMIM][2-CNpyr] and 0.1 M $TBAPF_6$ and 1 mM molecular catalyst when applicable. In the case of Ni(cyclam) Cl_2, a 5 mM stock solution of the compound in water was prepared. 1 ml of methanol was added to solubilize the catalyst . CVs with CO_2 were conducted by sparging solvent-saturated CO_2 into the electrolyte for 10 minutes. Controlled potential electrolysis experiments were performed in a custom H-cell with a 16 mL working compartment separated from an 8 mL counter compartment by a porous glass frit. The working and counter compartments were sealed using GL25 and GL18 open top caps with silicone/PTFE septa from Ace Glass. The working compartment containing the catholyte consisted of 1 mM molecular catalyst, 0.1 M IL, and 0.1 M $TBAPF_6$ in propylene carbonate. The counter compartment containing the anolyte had 0.1 M $TBAPF_6$ in propylene carbonate. For Fe(TPPS), the catholyte additionally included 0.1 M TFE as a proton source. For Ni(cyclam)Cl_2, the catholyte additionally included methanol (1.0 mL in the total of 10 mL catholyte) and water (1.8 mL in the total of 10 mL catholyte) as the proton source. Both systems used excess $Fe(C_5H_5)_2$ in the anolyte as a sacrificial reductant. The working electrodes were a 7/8" x 2.5" piece of carbon cloth purchased from Fuel Cell Earth. The reference electrode was a jacketed $Ag^{+/0}$ wire containing an electrolyte solution of 0.1 M $TBAPF_6$ in propylene carbonate. The counter electrode used the same carbon cloth as the working electrode in the case of Fe(TPPS), and Nichrome wire in the case of Ni(cylam)Cl_2 system, separated from the bulk solution by a porous Vycor frit. A Restek A-2 Luer lock gas-tight syringe was used to sample the headspace of the working compartment. Products were quantified using an Agilent 7890B GC instrument with a HP-PLOT molecular sieve column (19095P-MS6, 30 m x 0.530 mm, 25 μm) and thermal conductivity detector under helium carrier gas.

RESULTS AND DISCUSSION

Considerations for IL synthesis

As the halide impurity of the electrolyte is critical in electrochemical studies, careful monitoring of [EMIM][Br] conversion to [EMIM][OH] was performed by characterizing the solution after passing through the anion exchange column (flow rate of 3 mL/min and 3 grams of resin per millimole of starting halide) by NMR, FTIR, and ion chromatography for halide content. Another consideration besides the minimization of halide impurity was the reaction time for the follow-up metathesis step at 22 °C in methanol where the hydroxide and 2-CNpyrH neutralizes forming [2-CNpyr]$^-$ anion counter to the imidazolium cation and water as the side product. Figure S2 shows the evolution of the reaction in 1, 2, 3, 4, and 24 hrs as examined by ^{1}H-NMR. The reaction is fast and completes within 1 hr for both the 6- and 40-gram batches of ILs synthesized. The same conclusion was obtained by examining the FTIR spectra shown in Figure S3 for the sampled aliquots of the synthesis solution at the same time intervals.

It is common that one of the reagents is introduced in slight excess to push the equlibrium towards the syntheic products. In particular for this IL synthsis, the removal of the excess anion precursor is possible but not easy since it evaporates upon elevating the heating temperature under vacuum

https://doi.org/10.26434/chemrxiv-2023-tjz25 ORCID: https://orcid.org/0000-0003-4886-3350

which in turn color change in the liquid and attributed to possible degradation. To test whether the slight excess of the anion precuros can be justified in the light of this additional purification step, synthesis was performed with [EMIM][Br] to 2-CNpyrH molar ratios of 1:0.85, 1:1, and 1:1.2 for 1 hour. As seen from the NMR analysis shown in Figure S4a, the best composition is still 1:1. A 1:1 stoichiometry negates the necessity for subjecting the IL to elevated temperatures for extended periods, thus preventing the darkening of the IL in color and possible degradations[45].

Further, in the light of the varying affinities of anions on the strongly basic styrene-divinyl benzene type anion exchange resin we also assessed the anion exchange performance of [EMIM][Cl] as an alternative starting material to [EMIM][Br]. The proton integrations (Figure S4b) observed in the intermediates and the synthesized ILs from both precursors are consistent with each other and in line with the expected reaction stoichiometry. The results confirmed the absence of halides in both the 6 g and the 40 g batches of ILs synthesized, indicating the presented protocol in minimizing halide impurities in shortened reaction times.

Considerations for electrochemical characterization of IL electrolytes

Probing of the electrode-electrolyte interface through capacitance: Dynamic electrochemical impedance spectroscopy is a powerful tool that follows the evolving nature of electron transfer processes and double layer capacitance at charged interfaces. The impedance evolution during CO_2 electroreduction is outside the scope of this section, rather we will focus on the differential capacitance before active catalysis. Capacitance holds information on how the electrolyte-electrode interphase is structured and restructures with applied potential, and of course the chemical structure of the catalyst surface governs electrocatalytic activity. **Figure 2** shows the apparent catalytic activity of Ag with and without [EMIM][2-CNpyr] present, as well as the capacitance obtained from DEIS. The corresponding capacitance curves show drastic increase in

C_{dl} value upon IL addition. This is to be expected as tetrabutylammonium (TBA) cations do not densely adsorb at charged interfaces,[46-48] resulting in low surface capacitance on the order of 2-5 μF cm^{-2}. However, [EMIM] cations can reorient themselves to increase surface charge.[49] Here, the addition of the IL increases C_{dl} at potentials more positive than -0.6 V vs. Ag/AgCl from 2 to 10 μF cm^{-2}. We note that these results are different from standard differential capacitance measurements as they are not at steady state. The potential is actively sweeping which prevents cations from crowding and increasing the double layer thickness, thus resulting in increased C_{dl} values than expected.

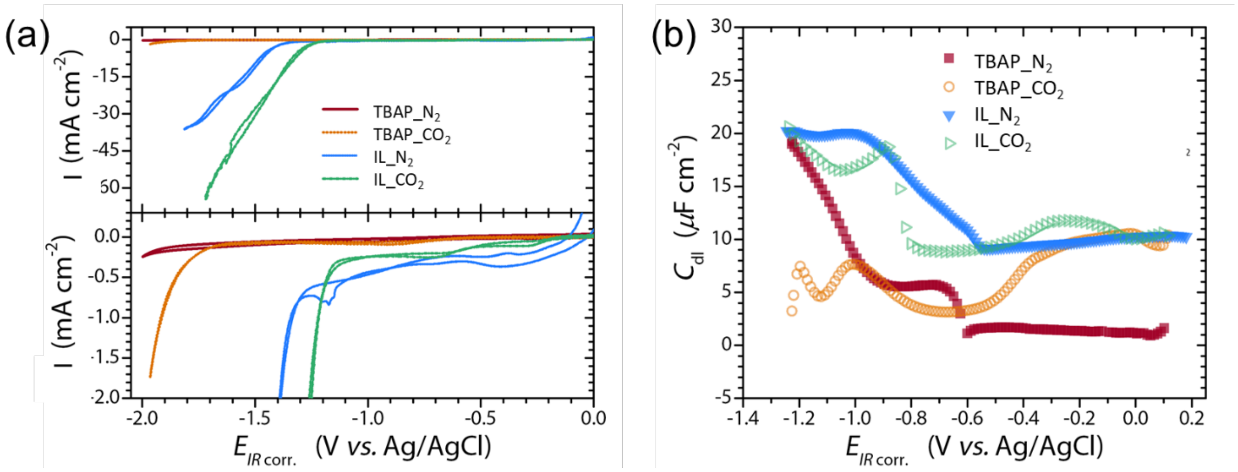

Figure 2: (a) CV curves recorded with Ag working electrode in N_2 and CO_2 saturated electrolytes containing 0.1 M TBAP /acetonitrile (red and orange) and 0.1 M [EMIM][2-CNpyr] added to 0.1 M TBAP/acetonitrile (blue and green) (CV scan rate- 10 mV/s); **(b)** differential capacitance curves obtained by fitting the time-resolved impedance data to a Randel's circuit to the higher frequency range (0.1 to 37.5 kHz).

CO_2 saturation further affects the C_{dl} profile more negative than -0.6 V vs. Ag/AgCl with and without the IL. Focusing on the potential range between -0.8 and -1.2 V when [EMIM][2-CNpyr] is present, the C_{dl} increase is delayed, shifting from -0.56 V in N_2 sat. to -0.79 V in CO_2 sat. V vs. Ag/AgCl. This result suggests that positive charges are blocked from the surface and indicative of adsorbed intermediates or spectators, which are then removed through sweeping in more negative direction. From NMR (Figure S5) we see CO_2 adducts of both $[EMIM]^+$-CO_2^- and [2-CNpyr]-CO_2. These species were observed via surface enhanced Raman spectroscopy adsorbed onto Cu catalyst.[13] Given that $[EMIM]^+$-CO_2^- is zwitterionic it is likely that this species is what impedes the capacitance and its dynamic reorientation and reduction results in a sharp capacitance increase.

Establishing the electrochemical stability and ECO_2R onset potential: ILs designed for specific applications such as ECO_2R are often synthesized in laboratories in very small quantities. Therefore, the initial assessment of their application performance and screening for a systematic set of structures necessitates minimization of sample volume. For determining electrochemical stability window, a T-cell setup has been used by many researchers[41, 44, 50] due to its microliter-sized sample requirement and ease of control in the environmental gas. **Figure 3a** shows the cyclic voltammetry curves obtained for [EMIM][2-CNpyr] by the T-cell shown in **Figure 1a**. It has been reported that the electrochemical stability window of ILs is constrained by the reduction potential of the cations and the oxidation potential of the anions. As shown in **Figure 3a**, exponential increase in the cathodic current was observed from -2.3 V (vs. Ag/Ag^+) under N_2, which can be attributed to the extensive reductive degradation of the [EMIM][2-CNpyr]. Additionally, the oxidation peak at 0.5 V is observed, which is mainly associated with pyrrolide anion oxidation.[51] In comparison, CO_2-saturated [EMIM][2-CNpyr] showed a very low current response, indicating an increased mass transport limitation due to the viscosity increase from 68 to 247 cP at 25 °C after CO_2 exposure.[36] This viscosity increase is a result of the interaction of the α-carbon on the imidazolium with CO_2 through the acidic hydrogen, as reported previously.[11] This is an important aspect of reactive ILs and necessitates proper *IR* correction[52] for not only an initial assessment on electrochemical stability windows but also the onset potential for electron transfer reactions.

Even though the use of microelectrode reduces the effect of diffusion limitations by changing the diffusion mode from linear to spherical and thereby reduce ohmic drop,[53] *IR* correction is still important. **Figure 3b** exemplifies the utilization of *IR* correction with a microelectrode for ECO_2R in a diluted IL electrolyte. Compensation for voltage drops is done by potentiostat by applying a high frequency ac perturbation (e.g., 100 kHz), which enables the measurement of only the uncompensated solution resistance. Correction allows for more accurate determination of the potential at the microelectrode-electrolyte interface. As shown in **Figure 3b**, the ECO_2R onset was observed at -1.85 V with no *IR* correction, and it shifts to -1.82 V after 85 % *IR* correction. Even though the potential shift is relatively small for the diluted electrolyte, the effect becomes more prominent with concentrated electrolytes or neat ILs. Another important aspect is the shielding that is needed, against external factors such as mechanical vibration and electrical noise present in the lab environment. Thus, the electrochemical cells equipped with microelectrodes should be placed inside a Faraday cage for prevention against external electromagnetic interferences that can distort the electrochemical signals (See Figure S6 for the impact of using a Faradic cage).

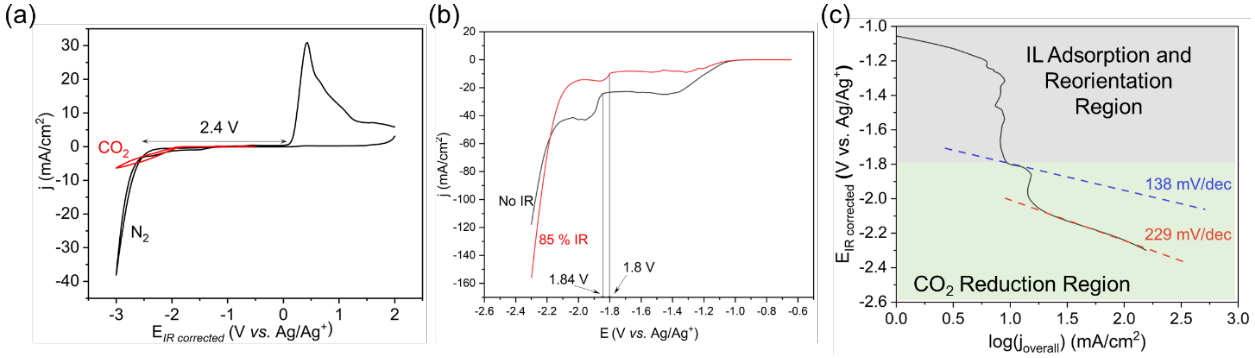

Figure 3: **(a)** Cyclic voltammetry of [EMIM][2-CNpyr] under N_2 (black) and CO_2 (red) sat. on Ag disk electrode (1.5 mm dia) with a scan rate of 10 mV/s, recorded using T-cell. The electrochemical window of 2.4 V was determined using a cutoff current density of 2 mA/cm^2; **(b)** LSV of CO_2 saturated 0.1 M [EMIM][2-CNPyr]/acetonitrile with 0.1 M TEAP supporting salt recorded using T-cell with Ag microelectrode (12.5 μm). The red and black curves represent LSV measurement performed with and without *IR* correction, showing positive shift in ECO_2R onset potential after *IR* compensation; **(c)** Tafel plot of ECO_2R in CO_2 saturated 0.1 M [EMIM][2-CNPyr]/acetonitrile with 0.1 M TEAP supporting salt. The Tafel plot is derived from the LSV measurement performed with Ag microelectrode with 85 % *IR* correction as shown in panel.

Examination of kinetics, solvent effects, and product selectivity: Similar to the difficulty in determining onset potential, the investigation of electron transfer kinetics is not straightforward with reactive ILs such as [EMIM][2-CNpyr]. It is known that ILs alter the electrode-electrolyte interfaces and form a unique double layer;[54] and reactive IL systems further present a dynamic behavior where conditions away from equilibrium. Therefore, it is not possible to determine which species are getting reduced at each potential, leading to limited linearity in Tafel slopes. **Figure 3c** shows an exemplary Tafel plot for [EMIM][2-CNpyr] obtained with microelectrode voltammetry. Throughout the polarization of the interface, IL cations absorb on the electrode surface, and change their orientation and lateral organization on the electrode surface,[13] which causes small current responses. In the ECO_2R region, the reduction starts with a Tafel slope of 138 mV/decade and the slope further increases to 229 mV/decade. This high value may suggest mass transport limitation or may be an indication of a small symmetry factor,[55] which is related to a large re-organizational energy penalty due to reduction reaction on the electrode. It is worth to note that, the changes in

Tafel slope occurs within a very short potential window (i.e., 200 mV), as seen in **Figure 3c** and the regions for the change in electrochemical reactions are distinct better seen in **Figure 3b**. These adsorption and double layer reorganization regions may not be distinguishable with macroelectrodes with large dispersion of electric field lines and catalytic sites, thus requiring careful analysis to relate observed kinetics between macro and microelectrodes.

In addition to kinetics, it is of interest to examine the product selectivity of the reduction reaction. Appreciable amounts of material are needed to reliably identify and quantify the products, which require high electrolyte conductivity to facilitate high currents. To overcome the innate high viscosity of ILs, dilution is required.[3, 41] Water as a dilutant introduces HER as a side reaction lowers the Faradaic efficiency (FE) toward ECO_2R products.[56] Moreover, water can lead to bicarbonate formation upon CO_2 exposure,[11, 36] which shifts effective pH and ultimately increases additional H_2 evolution during ECO_2R.[2] Therefore, we examined aprotic organic solvents and their effects on viscosity, conductivity, and the resulting current responses to identify suitable diluents for reactive ILs for reliable characterization of ECO_2R products as it has been shown that electrolyte effects are significant in ECO_2R.[34, 57]

Figure 4a shows how the viscosity and conductivity are improved by the various diluents. The corresponding LSVs in **Figure 4b** show that the choice of solvent significantly influences the CO_2 reduction onset potential, as well as the resulting CO_2 electroreduction activity. This difference can be attributed to several factors: ohmic drop induced by the lower ionic conductivity of electrolyte solutions composed of DMF (6.47 $mS.cm^{-1}$), DMSO (4.15 $mS.cm^{-1}$), NMP (2.85 $mS.cm^{-1}$), and PC (3.16 $mS.cm^{-1}$) which is a factor of 2 to 4 smaller than acetonitrile-based electrolyte (16.25 $mS.cm^{-1}$) (**Figure 4b**);[34, 57] effective CO_2 concentration (presented in **Table 1**), which includes speciation energetics and subsequent electrochemical activation; lastly, CO_2 diffusion which is governed by electrolyte viscosity.

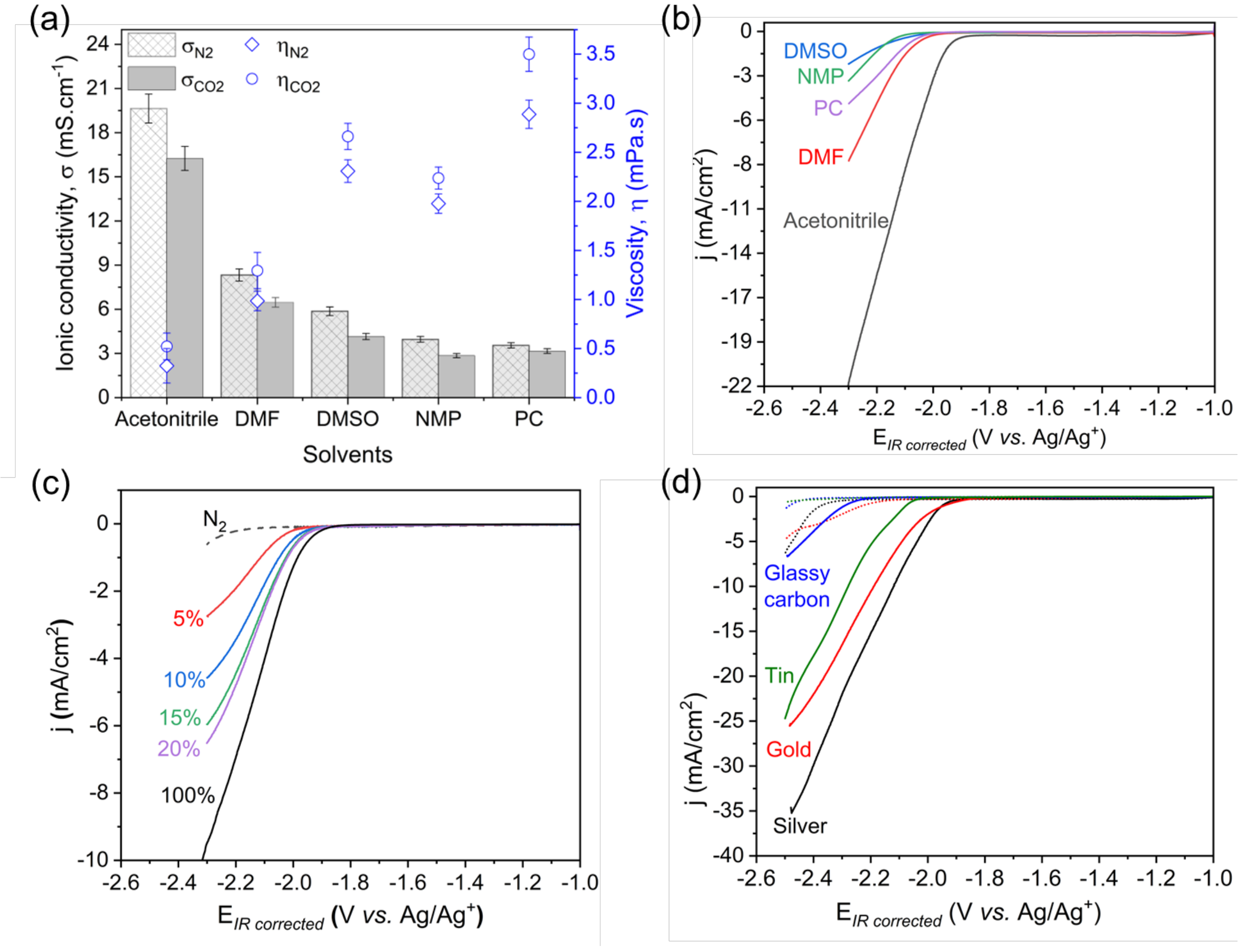

Figure 4: (a) Ionic conductivity (columns) and viscosity (circles) of 0.1 M IL electrolyte with various diluents at 25 °C; with N_2 (hollow) or CO_2 (filled) saturation; **(b)** LSVs with Ag electrode under CO_2 atmosphere; **(c)** LSV recorded with Ag disk working electrode showing effect of CO_2 partial pressure in feed gas on ECO_2R; and **(d)** LSV of the glassy carbon, gold, silver, and tin electrodes in N_2 (dotted line) and CO_2 (solid line) saturated 0.1 M [EMIM][2-CNpyr] showing the effect of electrode material on CO_2 reduction activity. LSVs were recorded in a single compartment electrochemical cell (electrolyte volume- 5 mL) at 10 mV/s scan rate and electrolyte

solutions composed of 0.1 M [EMIM][2-CNpyr] added to 0.1 M TEAP (supporting salt) in respective solvents.

While dilution is effective in enhancing ECO_2R rates, it is important to establish that the IL is still effective in terms of maintaining a high CO_2 solubility even when diluted. For physically absorbing ILs, the advantage of high CO_2 solubility is most likely lost when diluted, especially under low partial pressures of CO_2. However, reactive ILs present superior CO_2 capacities due to chemisorption. Figure S5 shows the quantitative ^{13}C NMR spectra 0.1 M and 1.5 M [EMIM][2-CNpyr] in acetonitrile, in comparison to the neat [EMIM][2-CNpyr] under N_2 and CO_2 saturation. It is determined that the same reaction products are present in both the diluted and neat samples, thus demonstrating the effectiveness of the CO_2-reactive IL even under dilution. The consideration for the right IL concentration should be based on the CO_2 source as much as the transport properties.[12, 13, 16] For instance, a higher IL concentration (e.g., 1.5 M for significant concentration of complexation sites) is suitable for low partial pressure of CO_2 and vice versa (e.g., 0.1 M for enhanced transport properties). **Figure 4c** shows the attainable current responses using Ag electrode with a 0.1 M IL in acetonitrile and 0.1 M tetrabutylammonium perchlorate (TEAP) as the supporting electrolyte, as a function of the CO_2 percentage in the feed gas (balanced with N_2). Controlling the partial pressure of CO_2 allows us to change the CO_2 concentration in the bulk electrolyte at room temperature.[36] As seen, increasing the CO_2 partial pressure leads to a shift in onset potential and increase in current density, capturing the expected relationship between the ECO_2R and the concentration of CO_2 in the electrolyte as it directly affects the near-surface concentration of CO_2.[58]

Finally, the effect of the heterogenous electrocatalyst was investigated in terms of the onset potential and current response for ECO_2R. **Figure 4d** shows the LSVs with Ag, Au, Sn, and glassy carbon (GC) electrodes in 0.1 M [EMIM][2-CNpyr] in acetonitrile with TEAP supporting salt, under N_2 and CO_2 purging conditions. In the N_2-purged electrolyte (indicated by the dashed line), the onset potential for the cathodic reaction was around -2.45, -2.3, -2.05, and -2.1 V vs. Ag/Ag^+ on glassy carbon electrodes, Ag, Sn, and Au, respectively. The majority of the reduction current was attributed to the degradation of [EMIM][2-CNpyr] itself, and the onset potential for the IL degradation varied depending on the electrode material. However, when the electrolyte was purged with CO_2 (illustrated by the solid line), the onset potential shifted towards more positive values: -2.25 V vs. Ag/Ag^+ on GC, -2.04 V vs. Ag/Ag^+ on Sn, and -1.89 V vs. Ag/Ag^+ on Ag and Au electrodes, respectively. This result suggests that the CO_2 reduction activity on the GC electrode is relatively low compared to Sn, Au, and Ag, thus confirming the heterogenous catalysis with the metal electrodes. The CO_2 reduction onset potential observed for Ag and Au are same, however, higher ECO_2R current was observed from -1.9 to -2.3 V (vs. Ag/Ag^+) with Ag electrode, indicating superior activity compared to Au. Because of high selectivity of CO on Ag, bulk electrolysis experiments were performed with Ag electrode in following section for simplicity.

ECO_2R activity was also studied in the presence of the molecular catalyst FeTPPS. Similar to the heterogeneous conditions described above, CV data of FeTPPS with 0.1 M [EMIM][2-CNpyr] in propylene carbonate shows an anodic shift in onset potential when purged with CO_2 (**Figure 5a**). Controlled potential electrolysis of this system at –2.5 V vs $Fe(C_5H_5)_2^{+/0}$ with 0.1 M TFE as a proton donor resulted in a linear increase of charge with time, passing –8.5 C of charge in 1 h (**Figure 5b**). The electrolysis exclusively produced CO with FE of 100%.

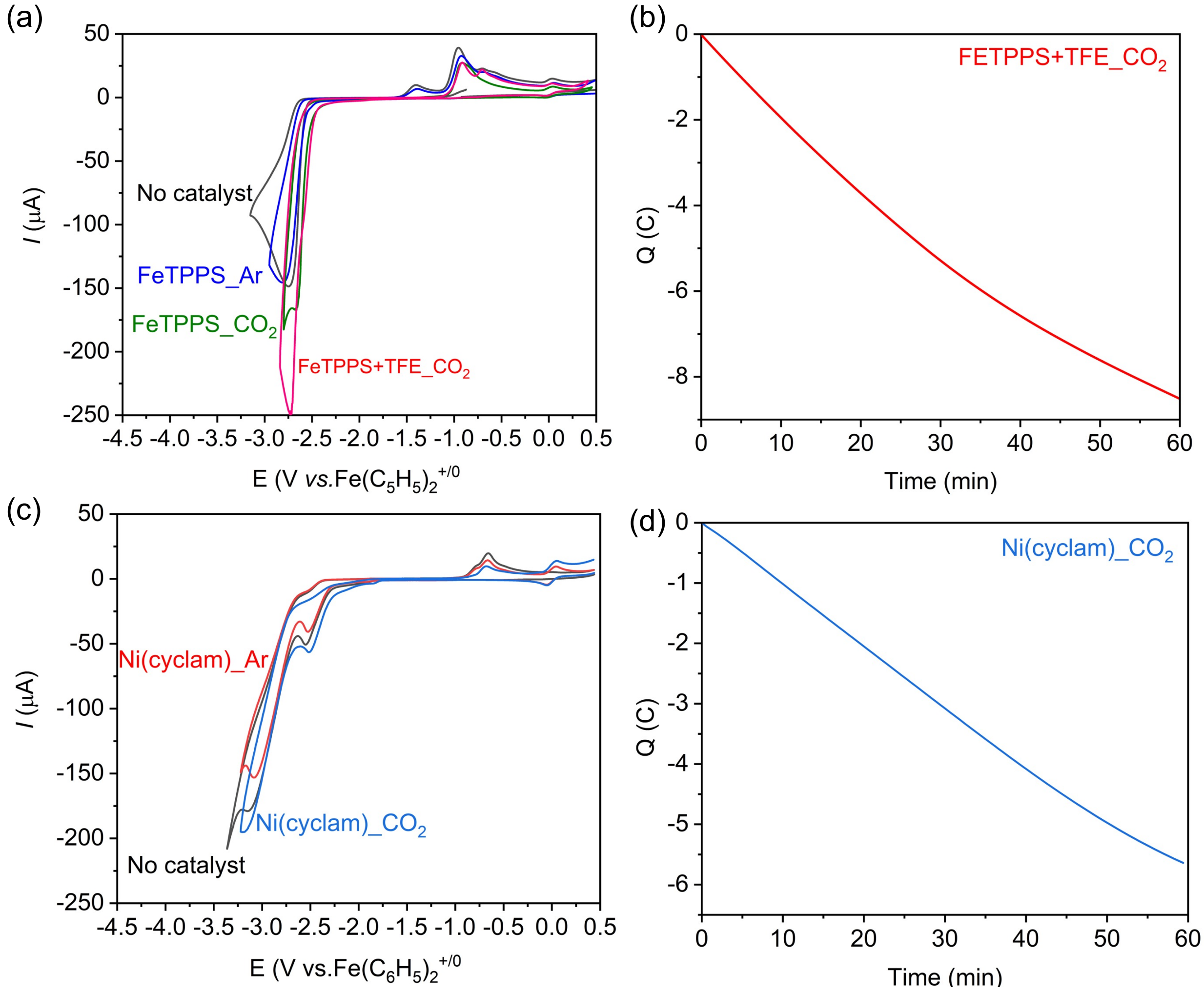

Figure 5: (a) CV data of 0.1 M [EMIM][2-CNpyr] in propylene carbonate (black) with 1 mM FeTPPS (blue). Saturation of CO_2 (green) and addition of 0.1 M TFE (red) result in a shift in the onset potential of [EMIM][2-CNpyr] reduction. **(b)** Controlled potential electrolysis of 1 mM FeTPPS with 0.1 M [EMIM][2-CNpyr] and 0.1 M TFE in propylene carbonate. **(c)** Shows CV response of 0.1M[EMIM][2-CNpyr] in propylene carbonate:water and MeOH (red trace), with the addition of Ni(cyclam)$^{2+}$ at 1mM (blue trace). Solution was saturated with CO_2 resulted in the current enhancement (green trace) All the CVs were recorded at 100 mV/s. **(d)** CPE data showing charge vs time plot with a potential held at -2.62 V vs Fc+/0 under same conditions as of cyclic voltammograms.

Figure 5c shows the cyclic voltammogram recorded in IL 0.1M[EMIM][2-Cypyr], and 1mM Ni(cyclam)$^{2+}$, The addition of CO_2 in presence of water and methanol shows a decrease in the cathodic potential with a simultaneous enhancement in the current, showing its catalytic activity for CO_2 reduction. CPE measurements carried out with a potential at -2.62 V vs $Fe(C_5H_5)_2^{+/0}$ under similar conditions showed linear accumulation of charge over time (**Figure 5d**) The gas product analysis of the headspace of the H-cell with a gas bridge showed HER and CO products with a FE of 14% and 79%, respectively.

Discussions on the choice of the reference electrode: Accurate and reproducible electrochemical measurements require well-defined and stable reference electrodes. However, most conventional reference electrodes are designed for aqueous systems, containing high concentrations of water and chloride.[59] In non-aqueous electrolysis studies, even trace amounts of water and chlorides can significantly impact electrochemical performance. Consequently, these reference electrodes are unsuitable for non-aqueous systems due to their anhydrous nature and the typical high concentration of chloride ions.[60] These findings have given rise to three main classes of reference electrodes used in non-aqueous media; pseudo, double junction, and soluble redox pairs[61] (see Figure S7). In many studies involving ILs, researchers have resorted to using "quasi-reference" or "pseudo-reference" electrodes. In these cases, a silver or platinum wire is immersed in the bulk electrolyte. Advantages of using these reference electrodes include decreased ohmic resistance, a negligible liquid junction potential, no contamination of solvent molecules or ions that an aqueous reference electrode might transfer, and no potential for frit pore plugging. However, these electrodes are often unreliable because their potential is influenced by impurities in the ILs or traces of oxides and other electrochemically active compounds on the electrode surface. Consequently, the reference potential can vary depending on the analyte, primarily due to differences in impurity solubilities and oxide compound presence. Even within the same sample, the potential can drift over time, especially after cleaning and polishing the pseudo-reference electrode.

The next class of reference electrodes involves the use of soluble redox pairs, this type of reference electrode is commonly used in aqueous media and includes Ag/AgCl and SCE.[62] These electrodes include a glass tube with a mounted frit that separates the redox pair from the main chamber of the cell. To modify these electrodes for use in non-aqueous media the solution within the reference electrode should be the same as the electrolyte in the cell with the addition of the desired redox pair. Advantages of using these types of reference electrode are specifically the elimination of water contamination as well as a liquid junction potential. The main disadvantage to this class of reference electrode is finding soluble and stable redox pairs in organic solvents. A redox pair that is frequently used in non-aqueous chemistry, especially within the field of ILs, is the silver-silver ion (Ag/Ag^+) electrode. It can be prepared by immersing a clean Ag wire into a solution containing 10 mM silver nitrate dissolved in 0.1 M tetraalkylammonium salts in acetonitrile.

Silver nitrate is soluble in a variety of organic solvents and the filling solution to the reference electrode should be constituted of the same solvent and electrolyte salt to avoid liquid junction potentials and ion contamination. It is important to note that this reference electrode is still susceptible to instabilities and proper maintenance of electrodes is key to reproducibility. It should be noted that, the reference potential of Ag/Ag^+ is strongly affected by presence of trace amount of water and the type of solvent used, as it changes the solvation of Ag^+ ion.[61] Therefore, a molecule with well-defined electrochemical behavior, such as ferrocene, can be added in very small amounts to the bulk electrolyte as an external reference.[63] The representative CV of Fc/Fc$^+$ redox behavior on Pt electrode is shown in Figure S8. However, issues can arise when the addition of internal reference redox couples leads to contamination of the working electrode, particularly when the redox potentials of the working electrode material and reference redox couples are closely aligned. This is particularly true in the case of Ag working electrode and the Fc/Fc$^+$ redox couple.[16] Further, other issues related to reference electrode's frit pore plugging (Figure S9) and Ag$^+$ ion leakage[64] are reported which interfere with the stability of reference electrode.[65] These interferences can be minimized by using double junction or salt bridge during the measurements(as shown in Figure S7). However, high electrode impedance due to the double junction need to be accounted during the measurements.

Approach to H-cell electrolysis for ECO$_2$R with IL electrolytes and interpretation of results: The methods described above are appropriate for screening of ILs and initial assessment of ECO$_2$R. However, these methods alone are not sufficient for further understanding of reaction products, Faradic efficiencies, and practical electrolyte stability. To decouple the interfacial reactions (e.g., ECO$_2$R *vs.* electrolyte degradation) at anode and cathode surfaces, the best next step is to performed an H-cell electrolysis experiment. In an H-cell where the anolyte and catholyte compartments were separated by a pretreated Nafion-117 membrane, electrolysis experiments were performed at -2.1 V (*vs.* Ag/Ag$^+$) for 1 hr with different combinations of electrode materials, electrolytes, and feed gases as summarized in **Table 2**. The resultant chronoamperometric curves are shown in Figure S10. These experiments were planned to study the effect of counter electrode material, electrolyte composition, and IL degradation on ECO$_2$R performance.

Table 2: Experimental conditions of the performed H-cell electrolysis to investigate the effect of electrode materials and electrolyte on product distribution and electrochemical stability. Total

charge (Q) is reported for 60 mins electrolysis at at -2.1 V (*vs.* Ag/Ag$^+$). Feed gas was consistently at 10 mL/min for both compartments. Cathodic chamber feed gas was CO_2 in all cases. Pictures in last column shows change in electrolyte color before and after electrolysis.

#	**Cathodic chamber**		**Anodic chamber**			Q (C)	Remarks
	Electrode	Electrolyte	Electrode	Electrolyte	Feed gas		
1	Ag	0.1 M TEAP	Pt	0.1 M TEAP	CO_2	2.18	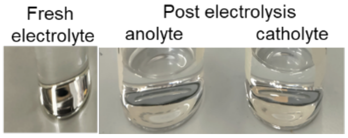
2	Ag	0.1 M IL	Pt	0.1 M IL	N_2	12.4	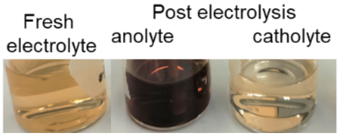
3				0.2 M TEAP	CO_2	12	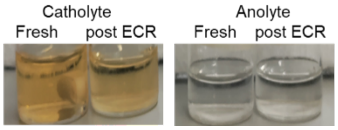
4	Ag	0.1 M IL	Carbon rod	0.1 M IL	CO_2	6.73	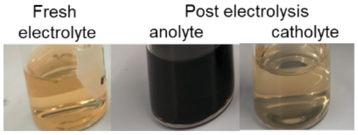
5			Pt	0.1 M 2-CNpyrH		12.3	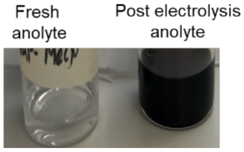 no color change with catholyte
6			Pt	0.1 M H_2SO_4		12.6	no color change with catholyte

To investigate the electrolyte composition, we initially performed electrolysis experiment with the use of 0.1 M TEAP/acetonitrile as the electrolyte in both compartments which resulted in 2.18 C charge utilization at -2.1 V (*vs.* Ag/Ag$^+$) in 1 hr of ECO_2R over Ag electrode. However, under the same experimental conditions, with the addition of 0.1 M IL, a sixfold increase in total charge utilization was observed. In both cases, only CO was detected in the gaseous product with a

Faradaic efficiency exceeding 95%. This increase in charge utilization can be attributed to the increased availability of CO_2 and the stabilization of reaction intermediates by the imidazolium cation.[12] To further investigate the changes occurring in the anolyte and catholyte, electrolytes were analyzed post-electrolysis using ^{1}H NMR spectroscopy and no changes were observed in the catholyte (Figure S11). Note that NMR is effective for measuring compounds that are 1wt % or higher in the liquid sample prepared. However, a few new peaks were detected in the anolyte (Figure S12), confirming the oxidative degradation of the IL at the Pt anode surface. Additionally, we observed a change in the color of the anolyte from light yellow to dark brown (as shown in Figure S12). Surprisingly, a similar anolyte degradation was observed when using a carbon rod anode, which is typically considered inactive for most electrochemical reactions. The appearance of new peaks in the ^{1}H NMR spectrum is attributed to the oxidative degradation (highlighted by the red arrow in Figure S12). The oxidative degradation of pyrrole compounds under the same applied potentials has been reported in the literature.[51] To further validate our findings, we performed an electrolysis experiment with the addition of 0.1 M 2-CNpyrH to the anode compartment. Same color change was observed, thus pointing to the likeliness of the pyrrole specie decomposition. Therefore, we conclude that IL should be avoided in the anolyte, especially when the IL contains a nucleophilic anion.

Most H-cell electrolysis experiments reported in the literature utilize aqueous anolyte solutions. Therefore, ECO_2R activity in the presence of 0.1 M H_2SO_4 on the anode side and non-aqueous 0.1 M [EMIM][2-CNpyr] on the cathode side was explored at -2.1 V vs. Ag/Ag^+ on Ag electrode. We observed a continuous increase in current over time. This was attributed to the exchange of hydrogen ions from the anolyte to the catholyte, resulting in excess HER. Gas product analysis confirmed H_2 evolution: the initially observed Faradaic efficiency for CO was 92% (over 20 minutes) decreased to 78% after 60 minutes (Figure S13). Hence, our findings highlight the importance of investigating the appropriate anolyte solution when employing IL as the active catholyte component in the combined capture and electrochemical conversion of CO_2.

CONCLUSION

An improved method of bulk synthesis of imidazolium cyanopyrrolide IL is presented in consideration of precursor composition and reaction for electrochemical studies. This refinement enhances the efficiency of scalable IL synthesis with minimized impurity. Furthermore, important considerations for studying homogeneous and heterogeneous electrocatalysis with ILs were discussed, using ECO_2R as a model reaction. The choice of catholyte solvent and the active electrode material has been shown to have significant influence on the activation overpotential for CO_2 reduction. Further, oxidative degradation of ILs has also been observed, emphasizing the need to avoid ILs specifically composed of nucleophilic anions in the anolyte. This study presents key considerations when evaluating electrolytes for reactive capture and electrochemical conversion of CO_2 in particular with nontraditional electrolytes containing functional ILs.

ACKNOWLEDGEMENT

This study was funded by the U.S. Department of Energy, Office of Science, Basic Energy Sciences, Energy Frontier Research Centers, under the grant awarded to Center for Closing the Carbon Cycle (4C) (DE-SC0023427).

AUTHORS CONTRIBUTION

S.D. performed electrochemical measurements, conducted gas and liquid analysis, and analyzed the data. E.C. optimized IL synthesis procedure. O.K.C. contributed to electrochemical measurements with microvoltammetry. J.S.S., A.Q.M., and J.Y.Y. carried out the measurements and analysis with the molecular catalysts. R.S.B. and J.M.V. contributed to the discussions related to suitable reference electrodes. R.L.S. performed dynamic electrochemical impedance spectroscopy measurements and analysis. B.G. conceived the project, conceptualized the study, and oversaw the progress. All the authors contributed to the discussions and edited.

REFERENCES

1. Goyal, A.; Marcandalli, G.; Mints, V. A.; Koper, M. T., Competition between CO2 reduction and hydrogen evolution on a gold electrode under well-defined mass transport conditions. *Journal of the American Chemical Society* **2020,** *142* (9), 4154-4161.
2. Moura de Salles Pupo, M.; Kortlever, R., Electrolyte effects on the electrochemical reduction of CO2. *ChemPhysChem* **2019,** *20* (22), 2926-2935.
3. Sullivan, I.; Goryachev, A.; Digdaya, I. A.; Li, X.; Atwater, H. A.; Vermaas, D. A.; Xiang, C., Coupling electrochemical CO2 conversion with CO2 capture. *Nature Catalysis* **2021,** *4* (11), 952-958.
4. Rosen, B. A.; Salehi-Khojin, A.; Thorson, M. R.; Zhu, W.; Whipple, D. T.; Kenis, P. J.; Masel, R. I., Ionic liquid–mediated selective conversion of CO2 to CO at low overpotentials. *Science* **2011,** *334* (6056), 643-644.
5. Zhigang Lei, B. C., Yoon-Mo Koo, and Douglas R. MacFarlane, Introduction: Ionic Liquids. *Chemical Reviews* **2017,** *117* (10), 6633-6635.

6. Schubert, T. J., Current and future ionic liquid markets. In *Ionic liquids: current state and future directions*, ACS Publications: 2017; pp 35-65.

7. Gordon, C. M.; Muldoon, M. J.; Wagner, M.; Hilgers, C.; Davis Jr., J. H.; Wasserscheid, P., Synthesis and Purification. In *Ionic Liquids in Synthesis*, 2007; pp 7-55.

8. Seo, S.; Quiroz-Guzman, M.; DeSilva, M. A.; Lee, T. B.; Huang, Y.; Goodrich, B. F.; Schneider, W. F.; Brennecke, J. F., Chemically Tunable Ionic Liquids with Aprotic Heterocyclic Anion (AHA) for CO2 Capture. *The Journal of Physical Chemistry B* **2014,** *118* (21), 5740-5751.

9. Blundell, R. K.; Licence, P., Quaternary ammonium and phosphonium based ionic liquids: a comparison of common anions. *Physical Chemistry Chemical Physics* **2014,** *16* (29), 15278-15288.

10. Lee, Y.-Y.; Gurkan, B., Graphene oxide reinforced facilitated transport membrane with poly(ionic liquid) and ionic liquid carriers for CO2/N2 separation. *Journal of Membrane Science* **2021,** *638*, 119652.

11. Lee, Y.-Y.; Edgehouse, K.; Klemm, A.; Mao, H.; Pentzer, E.; Gurkan, B., Capsules of reactive ionic liquids for selective capture of carbon dioxide at low concentrations. *ACS applied materials & interfaces* **2020,** *12* (16), 19184-19193.

12. Dongare, S.; Coskun, O. K.; Cagli, E.; Lee, K. Y.; Rao, G.; Britt, R. D.; Berben, L. A.; Gurkan, B., A Bifunctional Ionic Liquid for Capture and Electrochemical Conversion of CO2 to CO over Silver. *ACS catalysis* **2023,** *13*, 7812-7821.

13. Coskun, O. K.; Dongare, S.; Doherty, B.; Klemm, A.; Tuckerman, M.; Gurkan, B., Tailoring Electrochemical CO2 Reduction on Copper by Reactive Ionic Liquid and Native Hydrogen Bond Donors. *Angewandte Chemie International Edition n/a* (n/a), e202312163.

14. Wang, Y.; Hatakeyama, M.; Ogata, K.; Wakabayashi, M.; Jin, F.; Nakamura, S., Activation of CO 2 by ionic liquid EMIM–BF 4 in the electrochemical system: A theoretical study. *Physical Chemistry Chemical Physics* **2015,** *17* (36), 23521-23531.

15. Tanner, E. E.; Batchelor-McAuley, C.; Compton, R. G., Carbon dioxide reduction in room-temperature ionic liquids: the effect of the choice of electrode material, cation, and anion. *The Journal of Physical Chemistry C* **2016,** *120* (46), 26442-26447.

16. Liu, B.; Guo, W.; Gebbie, M. A., Tuning Ionic Screening to Accelerate Electrochemical CO2 Reduction in Ionic Liquid Electrolytes. *ACS Catalysis* **2022,** *12* (15), 9706-9716.

17. Sun, L.; Ramesha, G. K.; Kamat, P. V.; Brennecke, J. F., Switching the reaction course of electrochemical CO2 reduction with ionic liquids. *Langmuir* **2014,** *30* (21), 6302-6308.

18. Wuttig, A.; Surendranath, Y., Impurity ion complexation enhances carbon dioxide reduction catalysis. *ACS Catalysis* **2015,** *5* (7), 4479-4484.

19. Ma, C.; Laaksonen, A.; Liu, C.; Lu, X.; Ji, X., The peculiar effect of water on ionic liquids and deep eutectic solvents. *Chemical Society Reviews* **2018,** *47* (23), 8685-8720.

20. Guo, W.; Liu, B.; Gebbie, M. A., Suppressing Co-Ion Generation via Cationic Proton Donors to Amplify Driving Forces for Electrochemical CO2 Reduction. *The Journal of Physical Chemistry C* **2023,** *127* (29), 14243-14254.

21. Figueiredo, M. C.; Ledezma-Yanez, I.; Koper, M. T., In situ spectroscopic study of CO2 electroreduction at copper electrodes in acetonitrile. *Acs Catalysis* **2016,** *6* (4), 2382-2392.

22. Jang, J.; Rüscher, M.; Winzely, M.; Morales-Guio, C. G., Gastight rotating cylinder electrode: Toward decoupling mass transport and intrinsic kinetics in electrocatalysis. *AIChE Journal* **2022,** *68* (5), e17605.

23. Diercks, J. S.; Pribyl-Kranewitter, B.; Herranz, J.; Chauhan, P.; Faisnel, A.; Schmidt, T. J., An online gas chromatography cell setup for accurate CO2-electroreduction product quantification. *Journal of The Electrochemical Society* **2021,** *168* (6), 064504.

24. Wang, Y.; Hayashi, T.; He, D.; Li, Y.; Jin, F.; Nakamura, R., A reduced imidazolium cation layer serves as the active site for electrochemical carbon dioxide reduction. *Applied Catalysis B: Environmental* **2020,** *264*, 118495.

25. Pishgar, S.; Gulati, S.; Strain, J. M.; Liang, Y.; Mulvehill, M. C.; Spurgeon, J. M., In situ analytical techniques for the investigation of material stability and interface dynamics in electrocatalytic and photoelectrochemical applications. *Small Methods* **2021,** *5* (7), 2100322.

26. Iijima, G.; Kitagawa, T.; Katayama, A.; Inomata, T.; Yamaguchi, H.; Suzuki, K.; Hirata, K.; Hijikata, Y.; Ito, M.; Masuda, H., CO2 Reduction Promoted by Imidazole Supported on a Phosphonium-Type Ionic-Liquid-Modified Au Electrode at a Low Overpotential. *ACS Catalysis* **2018,** *8* (3), 1990-2000.

27. Katayama, Y.; Toshimitsu, Y.; Miura, T., Electrode kinetics of tris (2, 2′-bipyridine) ruthenium complexes in 1-ethyl-3-methylimidazolium tetrafluoroborate ionic liquid. *Journal of The Electrochemical Society* **2013,** *160* (4), H224.

28. Honores, J.; Quezada, D.; García, M.; Calfumán, K.; Muena, J.; Aguirre, M.; Arévalo, M.; Isaacs, M., Carbon neutral electrochemical conversion of carbon dioxide mediated by [M n+ (cyclam) Cl n](M= Ni 2+ and Co 3+) on mercury free electrodes and ionic liquids as reaction media. *Green Chemistry* **2017,** *19* (4), 1155-1162.

29. Grills, D. C.; Matsubara, Y.; Kuwahara, Y.; Golisz, S. R.; Kurtz, D. A.; Mello, B. A., Electrocatalytic CO2 reduction with a homogeneous catalyst in ionic liquid: high catalytic activity at low overpotential. *The Journal of Physical Chemistry Letters* **2014,** *5* (11), 2033-2038.

30. Froehlich, J. D.; Kubiak, C. P., Homogeneous CO2 Reduction by Ni(cyclam) at a Glassy Carbon Electrode. *Inorganic Chemistry* **2012,** *51* (7), 3932-3934.

31. Tarhini, A.; Aguirre-Araque, J.; Guyot, M.; Costentin, C.; Rogez, G.; Chardon-Noblat, S.; Prevot, V.; Mousty, C., Behavior of iron tetraphenylsulfonato porphyrin intercalated into LDH and LSH as materials for electrocatalytic applications. *Electrocatalysis* **2023,** *14* (1), 111-120.

32. Gennaro, A.; Isse, A. A.; Vianello, E., Solubility and electrochemical determination of CO2 in some dipolar aprotic solvents. *Journal of electroanalytical chemistry and interfacial electrochemistry* **1990,** *289* (1-2), 203-215.

33. Lide, D. R., *CRC handbook of chemistry and physics*. CRC press: 2004; Vol. 85.

34. Atifi, A.; Keane, T. P.; DiMeglio, J. L.; Pupillo, R. C.; Mullins, D. R.; Lutterman, D. A.; Rosenthal, J., Insights into the Composition and Function of a Bismuth-Based Catalyst for Reduction of CO2 to CO. *The Journal of Physical Chemistry C* **2019,** *123* (14), 9087-9095.

35. Kumar, A. S.; Pupo, M.; Petrov, K. V.; Ramdin, M.; van Ommen, J. R.; de Jong, W.; Kortlever, R., A Quantitative Analysis of Electrochemical CO2 Reduction on Copper in Organic Amide and Nitrile-Based Electrolytes. *The Journal of Physical Chemistry C* **2023,** *127* (27), 12857-12866.

36. Lee, Y.-Y.; Penley, D.; Klemm, A.; Dean, W.; Gurkan, B., Deep eutectic solvent formed by imidazolium cyanopyrrolide and ethylene glycol for reactive CO2 separations. *ACS Sustainable Chemistry & Engineering* **2021,** *9* (3), 1090-1098.

37. Kuwertz, R.; Kirstein, C.; Turek, T.; Kunz, U., Influence of acid pretreatment on ionic conductivity of Nafion® membranes. *Journal of Membrane Science* **2016,** *500*, 225-235.

38. Gurkan, B.; Goodrich, B.; Mindrup, E.; Ficke, L.; Massel, M.; Seo, S.; Senftle, T.; Wu, H.; Glaser, M.; Shah, J., Molecular design of high capacity, low viscosity, chemically tunable ionic liquids for CO2 capture. *The Journal of Physical Chemistry Letters* **2010,** *1* (24), 3494-3499.

39. McIntosh, A. J. S.; Griffith, J.; Gräsvik, J., Chapter 2 - Methods of Synthesis and Purification of Ionic Liquids. In *Application, Purification, and Recovery of Ionic Liquids*, Kuzmina, O.; Hallett, J. P., Eds. Elsevier: Amsterdam, 2016; pp 59-99.

40. Hugar, K. M.; Kostalik, H. A. I. V.; Coates, G. W., Imidazolium Cations with Exceptional Alkaline Stability: A Systematic Study of Structure–Stability Relationships. *Journal of the American Chemical Society* **2015,** *137* (27), 8730-8737.

41. Schröder, U.; Wadhawan, J. D.; Compton, R. G.; Marken, F.; Suarez, P. A.; Consorti, C. S.; de Souza, R. F.; Dupont, J., Water-induced accelerated ion diffusion: voltammetric studies in 1-methyl-3-[2, 6-(S)-dimethylocten-2-yl] imidazolium tetrafluoroborate, 1-butyl-3-methylimidazolium tetrafluoroborate and hexafluorophosphate ionic liquids. *New Journal of Chemistry* **2000,** *24* (12), 1009-1015.

42. Sacci, R. L.; Seland, F.; Harrington, D. A., Dynamic electrochemical impedance spectroscopy, for electrocatalytic reactions. *Electrochimica Acta* **2014,** *131*, 13-19.

43. Chen, C. S.; Handoko, A. D.; Wan, J. H.; Ma, L.; Ren, D.; Yeo, B. S., Stable and selective electrochemical reduction of carbon dioxide to ethylene on copper mesocrystals. *Catalysis Science & Technology* **2015,** *5* (1), 161-168.

44. Klein, J. M.; Squire, H.; Gurkan, B., Electroanalytical investigation of the electrode–electrolyte interface of quaternary ammonium ionic liquids: impact of alkyl chain length and ether functionality. *The Journal of Physical Chemistry C* **2019,** *124* (10), 5613-5623.

45. Lee, Y.-Y.; Cagli, E.; Klemm, A.; Park, Y.; Dikki, R.; Kidder, M. K.; Gurkan, B., Microwave Regeneration and Thermal and Oxidative Stability of Imidazolium Cyanopyrrolide Ionic Liquid for Direct Air Capture of Carbon Dioxide. *ChemSusChem n/a* (n/a), e202300118.

46. Han, T.; Park, M.-S.; Kim, J.; Kim, J. H.; Kim, K., The smallest quaternary ammonium salts with ether groups for high-performance electrochemical double layer capacitors. *Chemical Science* **2016,** *7* (3), 1791-1796.

47. Koh, A. R.; Hwang, B.; Roh, K. C.; Kim, K., The effect of the ionic size of small quaternary ammonium BF 4 salts on electrochemical double layer capacitors. *Physical Chemistry Chemical Physics* **2014,** *16* (29), 15146-15151.

48. Katakura, S.; Nishi, N.; Kobayashi, K.; Amano, K.-i.; Sakka, T., Effect of Switching the Length of Alkyl Chains on Electric Double Layer Structure and Differential Capacitance at the Electrode Interface of Quaternary Ammonium-Based Ionic Liquids Studied Using Molecular Dynamics Simulation. *The Journal of Physical Chemistry C* **2020,** *124* (14), 7873-7883.

49. Klein, J. M.; Panichi, E.; Gurkan, B., Potential dependent capacitance of [EMIM][TFSI],[N 1114][TFSI] and [PYR 13][TFSI] ionic liquids on glassy carbon. *Physical Chemistry Chemical Physics* **2019,** *21* (7), 3712-3720.

50. Li, P.; Barnes, E. O.; Hardacre, C.; Compton, R. G., Microelectrode Voltammetry of Dioxygen Reduction in a Phosphonium Cation-Based Room-Temperature Ionic Liquid: Quantitative Studies. *The Journal of Physical Chemistry C* **2015,** *119* (5), 2716-2726.

51. Bozzini, B.; Bocchetta, P.; Alemán, B.; Amati, M.; Gianoncelli, A.; Gregoratti, L.; Sezen, H.; Taurino, A.; Kiskinova, M., Electrodeposition and pyrolysis of Mn/polypyrrole nanocomposites: a study based on soft X-ray absorption, fluorescence and photoelectron microspectroscopies. *Journal of Materials Chemistry A* **2015,** *3* (37), 19155-19167.

52. Zheng, W., iR compensation for electrocatalysis studies: Considerations and recommendations. *ACS Energy Letters* **2023,** *8* (4), 1952-1958.

53. Stulík, K.; Amatore, C.; Holub, K.; Marecek, V.; Kutner, W., Microelectrodes. Definitions, characterization, and applications (Technical report). *Pure and Applied Chemistry* **2000,** *72* (8), 1483-92.

54. Fedorov, M. V.; Kornyshev, A. A., Ionic Liquids at Electrified Interfaces. *Chemical Reviews* **2014,** *114* (5), 2978-3036.

55. Gileadi, E.; Kirowa-Eisner, E., Some observations concerning the Tafel equation and its relevance to charge transfer in corrosion. *Corrosion science* **2005,** *47* (12), 3068-3085.

56. Ganji, P.; Borse, R. A.; Xie, J.; Mohamed, A. G. A.; Wang, Y., Toward commercial carbon dioxide electrolysis. *Advanced Sustainable Systems* **2020,** *4* (8), 2000096.

57. König, M.; Vaes, J.; Klemm, E.; Pant, D., Solvents and supporting electrolytes in the electrocatalytic reduction of CO2. *Iscience* **2019,** *19*, 135-160.

58. Moradzaman, M.; Martínez, C. S.; Mul, G., Effect of partial pressure on product selectivity in Cu-catalyzed electrochemical reduction of CO 2. *Sustainable Energy & Fuels* **2020,** *4* (10), 5195-5202.

59. Huber, B.; Roling, B., Development of a Ag/Ag+ micro-reference electrode for electrochemical measurements in ionic liquids. *Electrochimica Acta* **2011,** *56* (19), 6569-6572.

60. Shen, X.; Sinclair, N.; Wainright, J.; Akolkar, R.; Savinell, R., Evaluating and developing a reliable reference electrode for choline chloride based deep eutectic Solvents. *Journal of the Electrochemical Society* **2020,** *167* (8), 086509.

61. Izutsu, K., Reference electrodes for use in nonaqueous solutions. *Handbook of Reference Electrodes* **2013**, 145-187.

62. Smith, T. J.; Stevenson, K. J., 4 - Reference Electrodes. In *Handbook of Electrochemistry*, Zoski, C. G., Ed. Elsevier: Amsterdam, 2007; pp 73-110.

63. García Rey, N.; Dlott, D. D., Structural transition in an ionic liquid controls CO2 electrochemical reduction. *The Journal of Physical Chemistry C* **2015,** *119* (36), 20892-20899.

64. Leung, K. Y.; McCrory, C. C. L., Effect and Prevention of Trace Ag+ Contamination from Ag/AgCl Reference Electrodes on CO2 Reduction Product Distributions at Polycrystalline Copper Electrodes. *ACS Applied Energy Materials* **2019,** *2* (11), 8283-8293.

65. Roger, I.; Symes, M. D., Silver Leakage from Ag/AgCl Reference Electrodes as a Potential Cause of Interference in the Electrocatalytic Hydrogen Evolution Reaction. *ACS Applied Materials & Interfaces* **2017,** *9* (1), 472-478.